Journal of Molecular Catalysis B: Enzymatic 57 (2009) 299–303

Contents lists available at ScienceDirect

Journal of Molecular Catalysis B: Enzymatic

journal homepage: www.elsevier.com/locate/molcatb

Molecular modeling of substrate selectivity of *Candida antarctica* lipase B and *Candida rugosa* lipase towards *c*9, *t*11- and *t*10, *c*12-conjugated linoleic acid

Wencheng Li[a,1], Bo Yang[a,1], Yonghua Wang[b,*], Dongqing Wei[c], Chris Whiteley[d], Xiaoning Wang[a,*]

[a] *School of Bioscience and Bioengineering, South China University of Technology, Guangzhou 510641, China*
[b] *College of Light Industry and Food Sciences, Key Lab of Fermentation and Enzyme Engineering, South China University of Technology, Guangzhou 510641, China*
[c] *College of Life Science and Biotechnology, Shanghai Jiaotong University, Shanghai 200240, China*
[d] *Department of Biochemistry, Microbiology & Biotechnology, Rhodes University, Grahamstown 6139, South Africa*

ARTICLE INFO

Article history:
Received 20 April 2008
Received in revised form 7 October 2008
Accepted 8 October 2008
Available online 31 October 2008

Keywords:
Conjugated linoleic acid
Candida antarctica lipase B
Candida rugosa lipase
Substrate selectivity
Molecular modeling

ABSTRACT

Molecular modeling was used to clarify the mechanism of the selectivity of *Candida antarctica* lipase B and *Candida rugosa* lipase towards *cis*9, *trans*11 (*c*9, *t*11-) and *trans*10, *cis*12 (*t*10, *c*12-) conjugated linoleic acid. Hydrogen bonds network, substrate conformation, binding affinity and water molecules in the binding site were analyzed. Substrate conformation and binding affinity were not correlated with the experimental results of the substrate selectivity. On the contrary, better enzyme preference towards a substrate was correlated with two stronger hydrogen bonds (His-N_εH-O_a and His-N_εH-Ser-O_γ) and less water molecules between the substrate the binding pocket. Possible explanation of these was discussed.

1. Introduction

Lipases (EC 3.1.1.3) are diverse in their physical properties and substrate selectivities, which allow wide applications in industry. The substrate selectivities include stereo-, regio-, fatty acid and miscellaneous selectivities and these have been studied empirically and quantitatively. (i) Stereoselectivity: a rule, based on the size of the substituents at the stereocenter, was established to predict the enantioselectivity of cholesterol esterase, *Pseudomonas cepacia* lipase (PCL) and *Candida rugosa* lipase (CRL) towards secondary alcohols [1]. Quantitative models were established for predicting the enantioselectivity or stereoselectivity of enzymes. For example, a simple quantitative model was established for predicting the enantioselectivity of PCL, in which the distance between the catalytic histidine side chain and the alcohol oxygen $d(H_{N\varepsilon}\text{-}O_a)$ for the slow-reacting enantiomers in the productive binding mode was correlated with the enantioselectivity. Low and high *E*-values correlate to small and large $d(H_{N\varepsilon}\text{-}O_a)$ respectively [2]. Kahlow et al. discussed a similar model in CRL, in which the difference of $d(H_{N\varepsilon}\text{-}O_a)$ between the preferred and the nonpreferred enantiomer was correlated with the enantioselectivity [3]. Scheib et al. analyzed the stereoselectivity of *Rhizopus oryzae* lipase (ROL) and *Rhizomucor meihei* lipase (RML) towards triradylglycerols (*sn*-2 substituted triacylglycerols) [4,5]. They found that a single torsion angle ($\Phi_{O3\text{–}C3}$) was correlated to the *sn*-1 and *sn*-3 stereopreference and could serve as a simple model for predicting the stereoselectivity of new substrates. Haeffner et al. and Raza et al. used the potential energy of a number of subsets of the modeled system, calculated by molecular dynamics, to predict the enantioselectivity of *Candida antarctica* lipase B (CALB) towards secondary alcohols [6,7]. Molecular dynamics (MD), free energy perturbation (FEP) simulations, combined quantum mechanical/molecular mechanical (QM/MM) approaches were used to predict the enantioselectivity of subtilisin [8]. Water content was also found to be a determinant of enzyme enantioselectivity [9]. (ii) Regioselectivity: the regioselectivity of CALB, CRL and PCL towards cyclitol derivatives was explained by the favorable interactions or key hydrogen bonds for the favored catalyzed positions [10–12]. (iii) Fatty acid selectivity: attempts have been made to change the fatty acid selectivity of *Rhizopus delemar* lipase (RDL) towards short- or medium-chain length fatty acids by introduction of bulky hydrophobic residues or creating salt bridges

Abbreviations: CALB, *Candida antarctica* lipase B; CRL, *Candida rugosa* lipase; PCL, *Pseudomonas cepacia* lipase; ROL, *Rhizopus oryzae* lipase; RML, *Rhizomucor meihei* lipase; RDL, *Rhizopus delemar* lipase; CLA, conjugated linoleic acid; RMSD, root mean square displacement; MD, molecular dynamics; FEP, free energy perturbation simulations; QM/MM, combined quantum mechanical/molecular mechanical.

* Corresponding author. Tel.: +86 20 87113842; fax: +86 20 87113842.
E-mail address: xnwang@21cn.net (X. Wang).

[1] These authors participated equally to this work.

1381-1177/$ – see front matter © 2008 Published by Elsevier B.V.
doi:10.1016/j.molcatb.2008.10.009

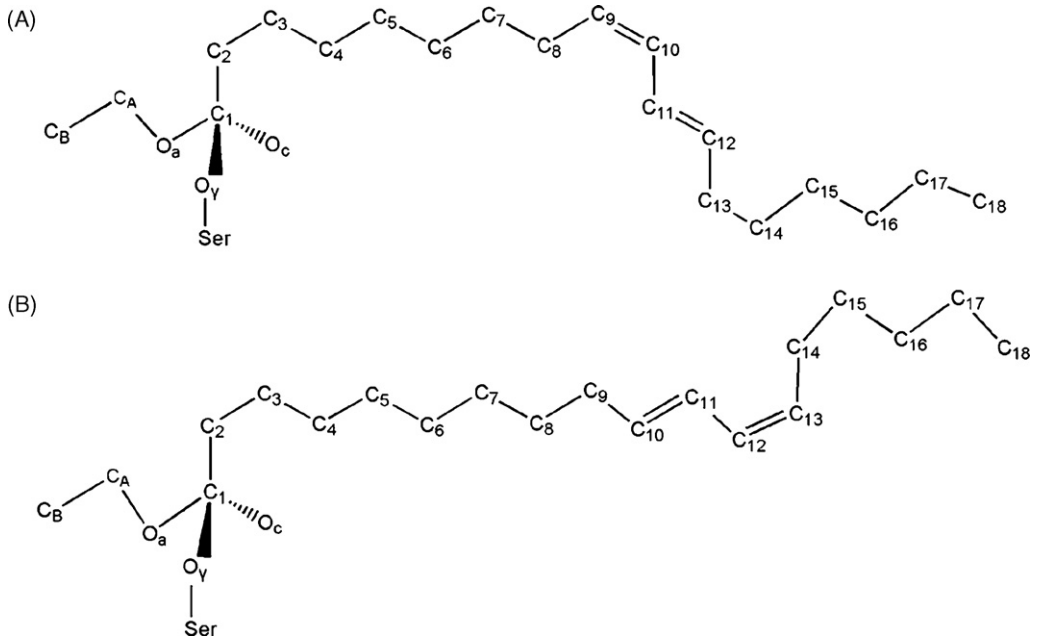

Fig. 1. The tetrahedral intermediate of ethyl esters of (A) *c*9, *t*11-CLA or (B) *t*10, *c*12-CLA with atom O_γ of the active site Serine of the enzyme. O_c and O_a are the carbonyl oxygen and alcohol oxygen of substrates respectively.

at discrete positions in the acyl binding groove guided by molecular modeling analysis [13]. (iv) Miscellaneous: Magnusson et al. made CALB to accommodate larger substituents other than an ethyl group in the stereospecific pocket by mutating Trp104 (the residue at the bottom of the stereospecific pocket) to Ala or Gln [14].

Conjugated linoleic acid (CLA) is a collective term that refers to a mixture of positional and geometrical isomers of linoleic acid with conjugated double bonds. The most commercially available CLA are all complex mixtures, of which *c*9, *t*11 and *t*10, *c*12-CLA (Fig. 1, abbreviated c9t11 and t10c12 respectively) are two major components present in almost equal amounts. Different isomers, however, have different bioactivities [15–17] and many attempts have been made to fractionate the CLA isomers [18–20]. We previously reported the selective esterification of c9t11 and t10c12 using CRL and CALB that had different selectivity on the two substrates. CRL catalyzed the esterification of c9t11 3.1–4.1 times faster than the corresponding reaction with t10c12, while CALB esterified t10c12 about 1.8–2 times faster than c9t11 [21]. To our knowledge, the molecular basis of this type of substrate selectivity is not well understood. CALB and CRL have funnel- and tunnel-like substrate binding site respectively [22], which may allow for different substrate selectivity. However, the conjugated double bonds are far away from the catalytic center. We now report on the use of molecular dynamics and molecular modeling to rationalize the question of how the different substrates have influenced the selectivity of the lipases. Furthermore this study may guide the actions of the fractionation of conjugated linoleic acid isomers catalyzed by lipases.

2. Experimental

2.1. Models for the reactive tetrahedral intermediates

The starting structures for molecular dynamics simulations were the crystal structure of CALB (pdb-entry 1LBS) [23] and the open form of CRL (pdb-entry 1LPO) [24]. Initially, the inhibitors and water molecules in the PDB structures were removed. The ethyl esters of *c*9, *t*11-CLA and *t*10, *c*12-CLA (Fig. 1) were then manually docked into the substrate-binding sites respectively. The initial location of the acyl groups of the substrates was guided by the conformation of the crystallographic inhibitors. The PDB structure files of the enzymes and the substrates were then converted into GROMACS format using program pdb2gmx in the GROMACS package version 3.3.3 [25,26] with GROMOS96 43a1 force field, and program PRODRG (http://davapc1.bioch.dundee.ac.uk/prodrg/index.html) [27] respectively. The files of the enzymes and the substrates in GROMACS format were then manually combined together. The H atoms of the Ser105-Oγ of CALB and Ser209-Oγ of CRL were replaced by covalent links to the tetrahedral C atom of the acyl moiety of

Table 1
Mulliken charges of the atoms in enzyme–substrate complex.

Atom[a]	Charges in complex			
	CALB-c9t11	CALB-t10c12	CRL-c9t11	CRL-t10c12
O_c	−0.661	−0.578	−0.597	−0.647
O_a	−0.188	−0.180	−0.149	−0.224
C_A	0.659	0.782	0.894	0.497
C_B	−0.366	−0.453	−0.337	−0.176
C_1	−0.820	−1.040	−1.405	−0.478
C_2	1.719	1.911	0.294	−0.057
C_3	−1.334	−1.538	0.663	0.638
C_4	0.429	0.395	−0.296	−0.431
C_5	−0.475	−0.681	−0.109	−0.063
C_6	0.030	0.182	−0.084	0.022
C_7	0.016	0.113	0.078	0.002
C_8	−0.090	−0.191	−0.239	0.021
C_9	0.227	−0.481	0.312	−0.270
C_{10}	−0.151	0.737	−0.086	0.102
C_{11}	−0.022	0.099	0.015	0.358
C_{12}	0.437	−0.256	0.513	−0.156
C_{13}	−0.267	0.177	−0.625	0.072
C_{14}	−0.186	−0.006	0.204	−0.085
C_{15}	0.039	−0.185	−0.181	−0.118
C_{16}	0.033	0.067	0.042	0.116
C_{17}	0.073	0.093	0.191	0.055
C_{18}	−0.102	−0.105	−0.195	−0.122
O_γ	−0.119	−0.032	−0.040	−0.036

[a] See Fig. 1 for the meaning of the name of every atom.

Table 2
Distances and angles of possible hydrogen bonds analyzed.

Id	Donor	Acceptor[a]	Distance (Å)[b]		Angle (°)[c]		Valid H-bonds (%)[d]	
			c9t11	t10c12	c9t11	t10c12	c9t11	t10c12
For CALB-substrates								
A1	Thr40-NH	O_c	1.8 ± 0.1	1.9 ± 0.2	164 ± 10	159 ± 14	99	98
A2	Thr40-O_γH	O_c	1.7 ± 0.1	1.8 ± 0.1	160 ± 10	156 ± 10	100	100
A3	Gln106-NH	O_c	1.8 ± 0.1	2.0 ± 0.1	168 ± 7	166 ± 8	100	100
A4	Gln106-$N_\varepsilon H_1$	O_c	4.0 ± 0.6	6.7 ± 0.6	121 ± 25	69 ± 18	17	0
A5	Gln106-$N_\varepsilon H_2$	O_c	5.0 ± 0.5	7.0 ± 0.6	58 ± 16	47 ± 16	0	0
A6	His224-N_εH	O_a	4.4 ± 0.2	3.9 ± 0.2	154 ± 8	143 ± 8	**0**	**3**
A7	Thr40-O_γH	O_a	2.3 ± 0.2	2.2 ± 0.2	135 ± 9	134 ± 8	95	96
A8	His224-N_εH	Ser105-O_γ	3.5 ± 0.3	2.7 ± 0.2	136 ± 6	125 ± 6	**46**	**79**
A9	His224-N_δH	Asp187-$O_\delta 1$	3.6 ± 0.4	5.0 ± 0.8	154 ± 11	110 ± 17	**26**	**0**
A10	His224-N_δH	Asp187-$O_\delta 2$	1.8 ± 0.2	5.1 ± 0.8	158 ± 12	107 ± 17	**99**	**0**
For CRL-substrates								
R1	Gly124-NH	O_c	1.9 ± 0.1	2.0 ± 0.2	165 ± 8	157 ± 9	100	100
R2	Ala210-NH	O_c	1.9 ± 0.2	2.0 ± 0.2	169 ± 7	163 ± 8	100	100
R3	Gly123-NH	O_c	1.8 ± 0.2	1.8 ± 0.1	160 ± 14	160 ± 10	**97**	**99**
R4	Ser209-NH	O_c	5.5 ± 0.2	5.2 ± 0.2	37 ± 8	36 ± 7	0	0
R5	His449-N_δH	O_a	5.6 ± 0.1	6.7 ± 0.4	24 ± 5	22 ± 9	0	0
R6	His449-N_εH	O_a	1.8 ± 0.1	3.5 ± 0.9	136 ± 5	116 ± 21	**100**	**36**
R7	Gly124-NH	O_a	2.9 ± 0.4	2.3 ± 0.2	139 ± 9	138 ± 9	**85**	**98**
R8	His449-N_εH	Ser209-O_γ	1.8 ± 0.1	2.4 ± 0.4	138 ± 5	139 ± 19	**100**	**82**
R9	His449-N_δH	Glu341-$O_{\varepsilon 1}$	1.7 ± 0.1	1.8 ± 0.3	170 ± 5	167 ± 7	**100**	**99**
R10	His449-N_δH	Glu341-$O_{\varepsilon 2}$	3.8 ± 0.1	3.2 ± 0.4	165 ± 6	143 ± 11	**1**	**74**

[a] O_c and O_a are the carbonyl oxygen and alcohol oxygen of substrates respectively.
[b] Distance is from donor hydrogen to acceptor. The mean values and the standard deviation of mean of the 1500–3000 ps trajectory are listed.
[c] Angle is donor–hydrogen–acceptor. The mean value and the standard deviation of mean of the 1500–3000 ps trajectory are listed.
[d] Percentage of valid hydrogen bond with distance <3.5 Å and angle >120°. Different values (Fisher's Exact test, $P < 0.01$) between the two complex are shown in bold.

each substrate. The His224 of CALB and His449 of CRL were protonated. The partial atomic charges (Table 1) of the substrates and the tetrahedral intermediate were determined by Mulliken population analysis using the DFT method implemented in the Gaussian 03, (Revision B.02) program [28] at the level of b3lyp/6-31+g(d). A box of Simple Point Charge water was added with a total size of 381 nm^3. To neutralize the system, 1 and 17 water molecule(s) beside CALB and CRL, respectively, was/were replaced by sodium ions at the positions with the most favorable electrostatic potential as determined by the program GENION in the GROMACS package. The systems were subjected to two rounds of steepest descent energy minimization (500 steps with the proteins frozen and another round of 500 steps with the backbone of the protein frozen) until the maximum force was less than 1.0 kJ/mol. Subsequent steepest descent minimization was carried out for 500 steps for all of the atoms in the system.

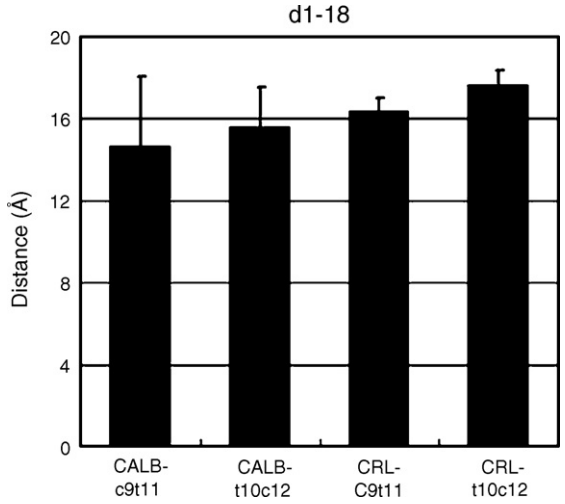

Fig. 2. Distance of C_1–C_{18} (d_{1-18}) of substrates. C_1 to C_{18} are carbon atoms of the acyl group of substrates starting from the carbonyl C atom. Error bar is standard deviation of mean.

2.2. Molecular dynamics simulation

The molecular dynamics simulations were carried out on a Computing Cluster using the program package GROMACS [25,26]. Periodic boundary conditions (PBC) were applied to all simulations performed and all the bond lengths were constrained applying the LINCS algorithm [29]. Nonbonded interactions were cut off after 10 Å, and the nonbonded interaction pair list was updated every 10 simulation steps. Starting velocities of atoms were generated according to a Maxwell distribution at a temperature of 300 K with a random seed. Molecular dynamics simulations were carried out at 300 K and 1 atm (total simulation time of 3000 ps with every step of 2 fs). Molecules were visualized using the VMD program [30]. If not stated, the 1500–3000 ps trajectory were used for the analysis.

3. Results and discussion

3.1. Analysis of the hydrogen bonds network

Each substrate has a carbonyl oxygen (O_c) and an alcohol oxygen (O_a) that could be stabilized by hydrogen bonds. It was reported that the O_c atom forms a negatively charged single-bonded oxyanion in the tetrahedral intermediate and is stabilized by hydrogen bonds in the oxyanion hole within the enzyme [7,31]. The distance between the O_a atom and the His449-N is a determinant of the enantioselectivity of CRL towards R- and S-enantiomers [3]. The catalytic triad (Ser-His-Asp/Glu) forms hydrogen bonds that are important for the catalytic activity of the lipases [7,31].

To elucidate the relationship of the hydrogen bond network and the selectivity of lipase towards different CLA esters, all possible hydrogen bonds with donors within 3.5 Å from O_c or O_a in the 1500–3000 ps trajectory, together with those important in the catalytic triad (listed in Table 2) were analyzed.

Table 3
List of interaction energies (kJ/mol) obtained by GROMACS.

	CALB-c9t11	CALB-t10c12	CRL-c9t11	CRL-t10c12
E (electronic)	−544 ± 89	−319 ± 61	−408 ± 38	−114 ± 31
E (van der Waals)	−65 ± 18	−8 ± 18	−128 ± 17	−159 ± 15
E (binding)	−610 ± 88	−327 ± 58	−536 ± 33	−273 ± 28

For CALB, the O_c atom is stabilized by Thr40-NH (A1), Thr40-O_γH (A2) and Gln106-NH (A3). Hydrogen bonds A1, A2 and A3 are similar with both the CALB–substrate complexes. A4 and A5 do not form stable hydrogen bonds as judged by the long distances (above 4 Å) and small angles (less than 120°). His224-N_εH may form weak hydrogen bonds (A6) with O_a as the distance is around 4 Å. The A6 of CALB-t10c12 (3.9 Å) is stronger than that of CALB-c9t11 (4.4 Å) since it has a shorter distance. Thr40-O_γH form strong and similar hydrogen bonds (A7) with O_a in both the CALB–substrate complexes. Hydrogen bonds of the catalytic triad (A8, A9 and A10) are quite different in the two CALB–substrate complexes. A8 is stronger in CALB-t10c12 and A9 and A10 are stronger in CALB-c9t11.

With respect to CRL, R1, R2 and R3 are similar between CRL-c9t11 and CRL-t10c12. R4 and R5 do not form hydrogen bonds as judged by the long distances (above 5 Å). R6 and R8 are stronger in CRL-c9t11 than CRL-t10c12, and R7 and R10 are stronger in CRL-t10c12 than CRL-c9t11.

In summary, two hydrogen bonds (A6 or R6, His-N_εH-O_a; A8 or R8, His-N_εH-Ser-O_γ) are correlated with the experiment results of Wang et al. [21] in which CALB and CRL favor t10c12 and c9t11 respectively, indicating that substrates with a stronger these two hydrogen bonds may be catalyzed more efficiently. The correlation between distance His-N_εH-O_a and substrates selectivity is consistent with a former study about the enantioselectivity of CRL towards R- and S-enantiomers [3]. The two hydrogen bonds were all very important in the catalytic process in which proton is transferred among atoms His-N_ε, O_a and Ser-O_γ [7]. A shorter distance of the two hydrogen bonds may accelerate the reaction.

3.2. Analysis of the substrate conformation

The geometry of the substrates was analyzed by calculating the distance between C_1 and C_{18} of the substrates (Fig. 2). Distance d_{1-18} is smaller in CRL-c9t11 (about 16 Å) than CRL-t10c12 (about 18 Å), indicating that c9t11 is more bent in CRL compared with t10c12. c9t11 is also more bent in CALB compared with t10c12, but d_{1-18} of CALB-substrates is more variable than that in CRL as indicated by the larger standard deviation value in CALB-substrates (Fig. 2). As c9t11 is more bent in both enzymes, the conformation of substrates may be not correlated with the substrates selectivity of the enzymes.

3.3. Analysis of the binding affinity

The binding energy of the two substrates with the two enzymes is shown in Table 3. Neither the electronic energy nor the van der Waals energy, nor the sum of them is correlated with the substrate

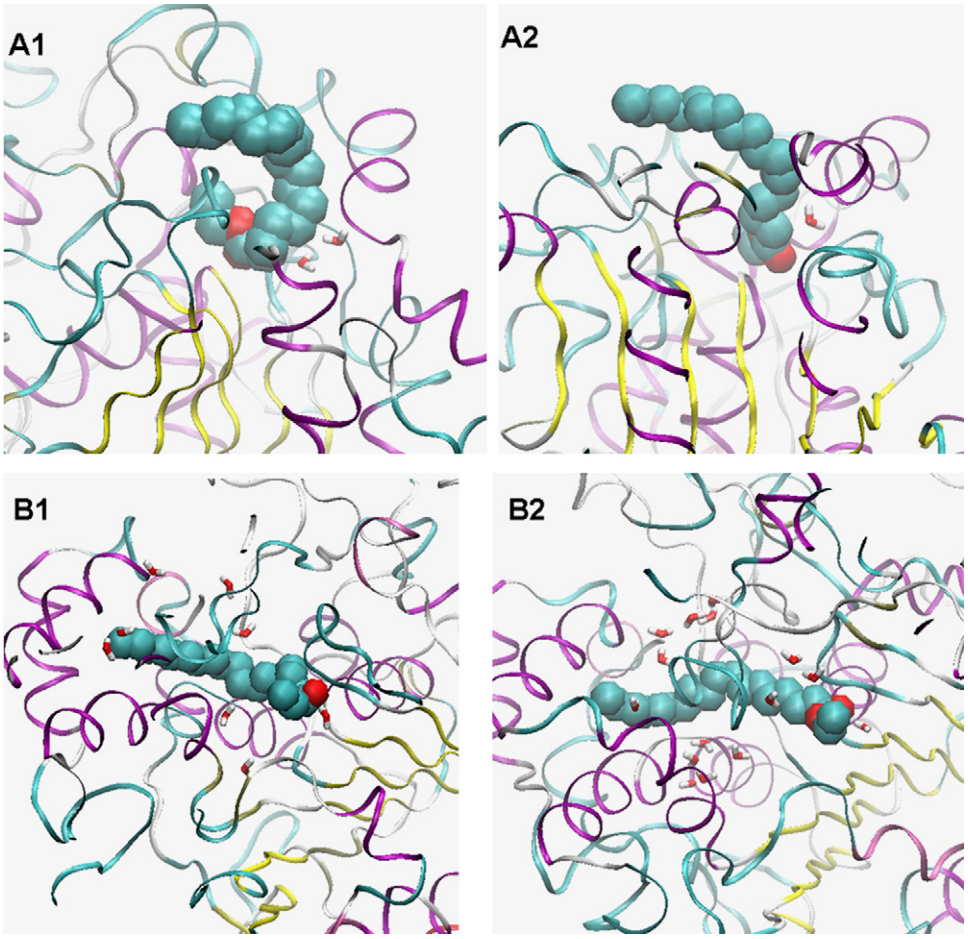

Fig. 3. Water molecules in the binding pockets of CALB-c9t11 (A1), CALB-t10c12 (A2), CRL-c9t11 (B1), CRL-t10c12 (B2). Enzymes, substrates and water molecules are shown as ribbons, space-filling and licorice respectively.

selectivity of the enzymes. c9t11 has lower binding energy with both the two enzymes. It indicates that the current energy items could not be an indicator of the selectivity of the enzymes. On the contrary, some key, specific interaction energy rather than the total binding energy might be more meaningful in predicting the selectivity of the enzymes.

3.4. Water moleculars in the binding pockets

It is reported that water molecular has a role in the substrates selectivity of enzymes [9]. Here, the water molecules in the binding site of the ultimate structures of the MD simulation were analyzed. As shown in Fig. 3, in CALB-substrates, half of the substrates (about atoms C_9–C_{18}) are out of the pocket of CALB. We analyzed water molecules within 5 Å of atom C_1–C_8, O_c, O_a, C_A and C_B of the substrates. Two water molecules are between c9t11 and the binding pocket of CALB and one for t10c12. As for CRL, Atoms C_3–C_{18} of the substrates are in the tunnel-like binding site of CRL. Water molecules within 7 Å of atoms C_3–C_{18} were analyzed. Eight water molecules are beside c9t11 and 14 beside t10c12.

It is interesting that the number of water molecules is correlated to the experiment results of selectivity (less water molecules correlated to higher enzyme preference towards a substrate). This may be explained by the following: (i) the acyl groups of substrates are mainly hydrophobic, thus the hydrophilic water may disturb the hydrophobic interactions between the binding pocket and the substrate; (ii) more water molecules mean larger space between the pocket and the substrate, indicating that the shape of the substrates and the pocket are not well fit.

4. Conclusions

Hydrogen bonds network, substrate conformation, binding affinity and water molecules in the binding site were analyzed to rationalize the question of how the different substrates have influenced the selectivity of the lipases. The two hydrogen bonds and the number of water molecules between the substrate and the binding pocket were correlated to the substrate selectivity. The strength of two hydrogen bonds (His-N_εH-O_a and His-N_εH-Ser-O_γ) may be two direct factors that influence the proton transfer in the catalytic process. On the other side, CALB has a funnel-like substrate binding pocket. Only about half-length of the substrates are interacted with the pocket. So the substrate selectivity of CALB may be less than CRL, which has a tunnel-like substrate binding site and the full acyl group are in the tunnel. The water molecules in the pocket may be an indicator of how the substrates are interacted with the pocket. More water molecules may mean that the substrate is not well bound or fit into the pocket.

Acknowledgements

This work was supported by the China Postdoctoral Science Foundation (20070410239) and the grants from National Natural Science Foundation of China (20506007 and 20706021) and the Research Fund for the Doctoral Program of Higher Education (20070561073). Additional support was from Computing Cluster of South China University of Technology.

References

[1] R.J. Kazlauskas, A.N.E. Weissfloch, A.T. Rappaport, L.A. Cuccia, J. Org. Chem. 56 (1991) 2656–2665.
[2] T. Schulz, J. Pleiss, R.D. Schmid, Protein Sci. 9 (2000) 1053–1062.
[3] U.H. Kahlow, R.D. Schmid, J. Pleiss, Protein Sci. 10 (2001) 1942–1952.
[4] H. Scheib, J. Pleiss, A. Kovac, F. Paltauf, R.D. Schmid, Protein Sci. 8 (1999) 215–221.
[5] J. Pleiss, H. Scheib, R.D. Schmid, Biochimie 82 (2000) 1043–1052.
[6] F. Haeffner, T. Norin, K. Hult, Biophys. J. 74 (1998) 1251–1262.
[7] S. Raza, L. Fransson, K. Hult, Protein Sci. 10 (2001) 329–338.
[8] G. Colombo, S. Toba, K.M. Merz, J. Am. Chem. Soc. 121 (1999) 3486–3493.
[9] N.M. Micaelo, V.H. Teixeira, A.M. Baptista, C.M. Soares, Biophys. J. 89 (2005) 999–1008.
[10] I. Lavandera, S. Fernandez, J. Magdalena, M. Ferrero, R.J. Kazlauskas, V. Gotor, Chembiochemistry 6 (2005) 1381–1390.
[11] C. Palocci, M. Falconi, S. Alcaro, A. Tafid, R. Puglisi, F. Ortuso, M. Botta, L. Alberghina, E. Cernia, J. Biotechnol. 128 (2007) 908–918.
[12] I. Lavandera, S. Fernandez, J. Magdalena, M. Ferrero, H. Grewal, C.K. Savile, R.J. Kazlauskas, V. Gotor, Chembiochemistry 7 (2006) 693–698.
[13] R.R. Klein, G. King, R.A. Moreau, M.J. Haas, Lipids 32 (1997) 123–130.
[14] B.A.O. Magnusson, J.C. Rotticci-Mulder, A. Santagostino, K. Hult, Chembiochemistry 6 (2005) 1051–1056.
[15] Y.L. Ha, J. Storkson, M.W. Pariza, Cancer Res. 50 (1990) 1097–1101.
[16] K. Nagao, N. Inoue, Y.M. Wang, J. Hirata, Y. Shimada, T. Nagao, T. Matsui, T. Yanagita, Biochem. Biophys. Res. Commun. 306 (2003) 134–138.
[17] K. Nagao, Y.M. Wang, N. Inoue, S.Y. Han, Y. Buang, T. Noda, N. Kouda, H. Okamatsu, T. Yanagita, Nutrition 19 (2003) 652–656.
[18] T. Kobayashi, T. Nagao, Y. Watanabe, Y. Yamauchi-Sato, S. Negishi, Y. Shimada, J. Am. Oil Chem. Soc. 83 (2006) 93–99.
[19] T. Nagao, Y. Yamauchi-Sato, A. Sugihara, T. Iwata, K. Nagao, T. Yanagita, S. Adachi, Y. Shimada, Biosci. Biotechnol. Biochem. 67 (2003) 1429–1433.
[20] Y. Yamauchi-Sato, T. Nagao, T. Yamamoto, T. Terai, A. Sugihara, Y. Shimada, J. Oleo Sci. 52 (2003) 367–374.
[21] Y.H. Wang, X.F. Li, Y.X. Liang, B. Yang, S.H. Zhang, J. Mol. Catal. B: Enzym. 46 (2007) 20–25.
[22] J. Pleiss, M. Fischer, R.D. Schmid, Chem. Phys. Lipids 93 (1998) 67–80.
[23] J. Uppenberg, N. Ohrner, M. Norin, K. Hult, G.J. Kleywegt, S. Patkar, V. Waagen, T. Anthonsen, T.A. Jones, Biochemistry 34 (1995) 16838–16851.
[24] P. Grochulski, F. Bouthillier, R.J. Kazlauskas, A.N. Serreqi, J.D. Schrag, E. Ziomek, M. Cygler, Biochemistry 33 (1994) 3494–3500.
[25] E. Lindahl, B. Hess, D. van der Spoel, J. Mol. Model 7 (2001) 306–317.
[26] D. Van Der Spoel, E. Lindahl, B. Hess, G. Groenhof, A.E. Mark, H.J. Berendsen, J. Comput. Chem. 26 (2005) 1701–1718.
[27] A.W. Schuttelkopf, D.M. van Aalten, Acta Crystallogr. D: Biol. Crystallogr. 60 (2004) 1355–1363.
[28] M.J. Frisch, G.W. Trucks, H.B. Schlegel, et al., Gaussian 03, Revision B.02, Gaussian Inc., Pittsburgh, PA, 2003.
[29] B. Hess, H. Bekker, H.J.C. Berendsen, J.G.E.M. Fraaije, J. Comp. Chem. 18 (1997) 1463–1472.
[30] W. Humphrey, A. Dalke, K. Schulten, J. Mol. Graph. 14 (1996) 33–38.
[31] M. Cygler, J.D. Schrag, Biochim. Biophys. Acta 1441 (1999) 205–214.